Chapter 15 | Agricultural and Forest Micrometeorology

15.1 Flux-profile Relations above Plant Canopies

In this final chapter we discuss the particular applications of micrometeorological principles and methods to vegetative surfaces, such as agricultural crops, grasslands, and forests. Here, the micrometeorologist is interested in the atmospheric environment, both above and within the plant canopies, as well as in the complex interactions between vegetation and its environment. First, we discuss the vertical profiles of mean wind, temperature, specific humidity, etc., and their relationships to the vertical fluxes of momentum, heat, water vapor, etc., above plant canopies.

The semiempirical flux-profile relations developed in Chapters 10–12 should, in principle, apply to any homogeneous surface layer, well above the tops of roughness elements ($z > h_0 \gg z_0$). It should be kept in mind, however that for any tall vegetation the apparent reference level for measuring heights must be shifted above the true ground level by an amount equal to the zero-plane displacement (d_0), which is related to the mean height (h_0) of roughness elements and roughness density. Also, for flexible plant canopies, z_0 and d_0 may not have fixed ratios to h_0 but may vary with wind speed. Physically, one can argue that for a vegetative canopy acting as a sink of momentum and a source or sink of heat, water vapor, CO_2, etc., the effective source or sink height must lie between $0.5h_0$ and h_0. For exchange processes in the atmospheric boundary layer well above the canopy, it is found convenient to consider the canopy as an area source or sink of infinitesimal thickness located at an effective height d_0 above the ground level, and to consider it an effective reference plane. Then, the zero-plane displacement does not appear explicitly in theoretical or semiempirical flux-profile relations, such as those given in Chapters 10–12. In most experimental situations and practical applications, however, the ground level is the most convenient reference plane for measuring heights. It is also the appropriate reference plane for representing mean and turbulent quantities within the canopy layer. For these reasons, in this chapter, we will use the height z above the local ground level and account for the zero-plane displacement, wherever appropriate (e.g., in the above-canopy flux-profile relations).

Applying the Monin–Obukhov similarity theory to the fully-developed part of the constant-flux surface layer, also called the 'inertial sublayer', in which the flux-profile relations are expected to have the same forms as in the idealized surface layer over low roughness, we can rewrite Equation (11.2) as

$$\begin{aligned} \frac{k(z-d_0)}{u_*}\frac{\partial U}{\partial z} &= \phi_m(\zeta) \\ \frac{k(z-d_0)}{\theta_*}\frac{\partial \Theta}{\partial z} &= \phi_h(\zeta) \\ \frac{k(z-d_0)}{q_*}\frac{\partial Q}{\partial z} &= \phi_w(\zeta) \end{aligned} \tag{15.1}$$

where $\zeta = (z - d_0)/L$ is the M–O stability parameter. As shown earlier in Chapters 11 and 12 the integral forms of Equation (15.1) represent the mean wind speed, potential temperature, and specific humidity profiles in the similarity forms as

$$\begin{aligned} \frac{U}{u_*} &= \frac{1}{k}\left[\ln\left(\frac{z-d_0}{z_0}\right) - \psi_m\left(\frac{z-d_0}{L}\right)\right] \\ \frac{\Theta-\Theta_0}{\theta_*} &= \frac{1}{k}\left[\ln\left(\frac{z-d_0}{z_0}\right) - \psi_h\left(\frac{z-d_0}{L}\right)\right] \\ \frac{Q-Q_0}{q_*} &= \frac{1}{k}\left[\ln\left(\frac{z-d_0}{z_0}\right) - \psi_w\left(\frac{z-d_0}{L}\right)\right] \end{aligned} \tag{15.2}$$

where Θ_0 and Q_0 are the values at $z = d_0 + z_0$, and θ_* and q_* are the scaling parameters, each representing the ratio of the appropriate vertical flux (in kinematic units) to the friction velocity u_* [Equation (12.12)]. The M–O similarity functions ψ_h and ψ_w are presumably equal, but may differ from the momentum function ψ_m, especially in unstable and free convective conditions. The empirical forms of these functions over homogeneous land surfaces with short roughness including vegetation, as well as water surfaces, have already been discussed in Chapters 11 and 12.

The gradient and bulk parameterizations of the vertical fluxes of momentum, heat, etc., in an idealized (constant-flux, horizontally homogeneous, stationary) surface layer have also been discussed in Chapters 11 and 12. These can be applied to the above-canopy inertial sublayer, especially in the height range $0.1h > z > 2h_0$. The range of validity of the surface layer similarity relations becomes narrower for taller canopies and for shallow boundary layers. It may

disappear completely when the PBL thickness is less than 10–15 times the vegetation height, a distinct possibility over mature forest canopies.

15.1.1 Profile relations in the roughness sublayer

Even when allowance is made for the zero-plane displacement, significant deviations from the log law under neutral conditions and the more general M–O similarity profiles given in Equation (15.2) under stratified conditions have been observed to occur in the so-called roughness sublayer which is a transition layer between the canopy layer below and the constant-flux inertial sublayer above (see also Garratt, 1992, Chapter 3). This roughness transition layer is characterized by relatively small values of $(z - d_0)/z_0$, ranging between 10 and 150. It has been found from micrometeorological measurements over tall crops and forests that the dimensionless similarity functions ϕ_m, ϕ_h, etc., attain their expected surface-layer similarity forms only above a certain minimum height z_* which is estimated to be 1.5 to 2.5 times the average height of roughness elements (i.e., $z_*/h_0 = 1.5$–2.5). In terms of the roughness length/parameter, $(z_* - d)/z_0$ has been estimated to vary between 10 and 150. Thus, the roughness-sublayer thickness may vary from less than a meter over short vegetation to several tens of meters over forest canopies.

Due to enhanced turbulent mixing in the roughness sublayer, dimensionless wind shear and vertical gradients of temperature and specific humidity are found to be significantly reduced from their equilibrium values in the inertial sublayer or the idealized surface layer over low roughness for the same value of $(z - d_0)/L$ (Raupach, 1979; Garratt, 1980; Hogstrom *et al.*, 1989). In particular, the large (up to 75%) reduction in the dimensionless gradient of potential temperature seems to be a universal finding over forest canopies. The reduction in the dimensionless wind shear appears to be related in some way to the density of canopy (Hogstrom *et al.*, 1989). Significant reductions (up to 65%) of ϕ_m have been observed over sparse Savannah and other forests, but not over dense forests. The dimensionless specific humidity gradient (ϕ_w) also shows strong reduction in the roughness sublayer, particularly just above the treetops. The ratio ϕ_w/ϕ_h is found to be about one under unstable conditions, but somewhat larger (about 1.4) under near-neutral conditions. It should be recognized, however, that it is not easy to measure ϕ_h accurately enough under near-neutral conditions when both $\partial\Theta/\partial z$ and θ_* tend to zero.

A somewhat controversial finding by some investigators is that the ratios between the measured dimensionless gradients in the roughness sublayer and their expected values in the idealized surface layer over low roughness are more or less independent of stability. The suggested modified similarity relations that

account for the observed reductions of dimensionless gradients in the roughness sublayer are

$$\begin{aligned}
\frac{k(z-d_0)}{u_*}\frac{\partial U}{\partial z} &= \phi_m(\zeta)\phi_m^*(\eta) \\
\frac{k(z-d_0)}{\theta_*}\frac{\partial \Theta}{\partial z} &= \phi_h(\zeta)\phi_h^*(\eta) \\
\frac{k(z-d_0)}{q_*}\frac{\partial Q}{\partial z} &= \phi_w(\zeta)\phi_w^*(\eta)
\end{aligned} \tag{15.3}$$

in which the reduction factors $\phi_m^*(\eta)$, etc., are assumed to be functions of the normalized height parameter $\eta = (z-d)/(z_*-d)$ only, independent of stability. For sparse forest canopies, Garratt (1992) has suggested a simple empirical form for all the reduction factors $\phi_m^* \cong \phi_h^* \cong \phi_w^* = \phi^*$:

$$\phi^*(\eta) = \exp[-0.7(1-\eta)], \quad \text{for } \eta \leq 1 \tag{15.4}$$

It should be recognized, however, that over dense forest canopies, the empirical constants may be different for different reduction functions when they are represented by similar exponential expressions as Equation (15.4). The top of the roughness sublayer (height z_*) can be estimated in terms of the average height of the dominating trees (e.g., $z_* = 1.5h_0$ to $2.5h_0$, depending on the roughness density).

The similarity functions ψ_m, ψ_h, etc., in the profile equations (15.2) should also be modified in the roughness sublayer in accordance with the flux-gradient relations (15.3). Other parameters most directly affected by the reductions in ϕ_m, ϕ_h, etc., are the eddy diffusivities K_m, K_h, etc., which have been observed to increase in the roughness sublayer. The enhancement of eddy diffusivities is expected to be inversely proportional to $\phi^*(\eta)$. The suggested mechanisms for the enhancement of turbulent exchanges in the roughness sublayer are the wakes generated by roughness elements and thermals rising between individual elements (Monteith and Unsworth, 1990, Chapter 14).

15.1.2 Transfer coefficients and resistances

The flux parameterizations that employ the drag coefficient and other transfer coefficients are commonly used in micrometeorology and its applications to air–sea interaction, air pollution, hydrology, large-scale atmospheric modeling, etc. In these, the various fluxes are linearly related to the products of wind speed and

the difference between the values of variables at some reference height in the surface layer and at the surface itself. For example

$$\begin{aligned} \tau_0 &= \rho C_D U^2 \\ H_0 &= \rho c_p C_H U(\Theta_0 - \Theta) \\ E_0 &= \rho C_W U(Q_0 - Q) \end{aligned} \tag{15.5}$$

in which the drag coefficient (C_D) and other transfer coefficients can be prescribed as functions of the surface roughness (more appropriately, $(z - d)/z_0$) and stability (e.g., Ri_B) parameters, as discussed in Chapter 11. On the basis of Reynolds analogy (similarity of transfer mechanisms of heat, water vapor, etc.), one expects that $C_H = C_W$.

Another commonly used approach or method of parameterizing the vertical fluxes in terms of the difference in mean property values at two heights is the 'aerodynamic resistance' approach, which is based on the analogy to electrical resistance and Ohm's law:

$$\text{current} = \frac{\text{potential difference}}{\text{electrical resistance}}$$

The analogous relations for turbulent fluxes are

$$\begin{aligned} \tau_0 &= \rho r_M^{-1} U \\ H_0 &= \rho c_p r_H^{-1}(\Theta_0 - \Theta) \\ E_0 &= \rho r_w^{-1}(Q_0 - Q) \end{aligned} \tag{15.6}$$

in which r_M, r_H, etc., are the aerodynamic or aerial resistances to the transfer of momentum, heat, etc. Note that a flux will increase as the appropriate aerodynamic resistance decreases. In engineering literature, transfer coefficients having the dimensions of velocity are used, instead of inverse resistances, in empirical parameterizations of fluxes.

The resistance approach is more frequently used in micrometeorological applications in agriculture and forestry. This is largely because of the simple additive property of resistances in series, which can be used to express the total aerodynamic resistance in terms of resistances of its components (bare soil surface, leaves, branches, and stems of plants). A disadvantage is that, unlike the dimensionless transfer coefficients, aerodynamic resistances are dimensional properties, having dimensions of the inverse of velocity, which depend not only on the canopy structure, but also on the wind speed at the appropriate height and atmospheric stability. Also, in practice, it is not easy to determine and

specify the component resistances for estimating the overall canopy resistance. A comparison of Equations (15.5) and (15.6) clearly shows that the bulk transfer method is superior to the aerodynamic resistance method, but the two sets of coefficients are interrelated as

$$r_M^{-1} = UC_D; \quad r_H^{-1} = UC_H; \quad r_w^{-1} = UC_W \tag{15.7}$$

Thus, for a given canopy, aerial resistances are inversely related to wind speed and are not unique properties of canopy and the surface. The reciprocals of resistances may also be called transfer velocities or conductances. The deposition velocity of a gaseous pollutant is often parameterized in terms of the aerodynamic and other resistances (Arya, 1999, Chapter 10).

15.2 Radiation Balance within Plant Canopies

Solar or shortwave radiation is the main source of energy for the vegetation. Longwave radiation is also a major component of energy balance in daytime and the primary component at nighttime. In plant canopies radiation has important thermal and photosynthetic effects; it also plays a major role in plant growth and development processes. The visible part of the shortwave radiation (0.38–0.71 μm) is called the photosynthetically active radiation (PAR).

Radiative transfer in a plant canopy is a very complicated problem for which no satisfactory general solution has been found. There are significant amounts of internal radiative absorption, reflection, transmission, and emission within the canopy elements. Complications also arise from the large variability and inhomogeneity of the canopy architecture, as well as of individual plants. The canopy architecture also determines, to a large extent, the turbulent exchanges of momentum, heat, water vapor, CO_2, etc., within the canopy and is discussed briefly in the following section.

15.2.1 Canopy architecture

The size and shape of canopy elements, as well as their distributions in space and time, determine the physical characteristics of the canopy structure. A detailed description of a nonhomogeneous or nonuniform plant canopy in a complex terrain would necessarily involve many parameters. A commonly accepted simplification is made by assuming that the plant stand is horizontally uniform and its average characteristics may vary only with height above the ground.

The simplest characteristic of the canopy structure is its average height or thickness h_0. Along with the area density of the plants, h_0 determines the roughness parameter and the effective heights of the sources or sinks of momentum, heat, moisture, etc. Another widely used characteristic of the canopy architecture is the cumulative leaf area index (L_{AI}), defined as the area of the upper sides of leaves within a vertical cylinder of unit cross-section and height h_0. The leaf area index is a dimensionless parameter which is related to the foliage area density function $A(z)$ as (Ross, 1975)

$$L_{AI} = \int_0^{h_0} A(z)dz \tag{15.8}$$

Here, $A(z)$ is a local characteristic of the canopy architecture which represents the one-sided leaf area per unit volume of the canopy at the height z. A more convenient dimensionless local characteristic is the local cumulative leaf area index

$$L_{AI}(z) = \int_z^{h_0} A(z)dz \tag{15.9}$$

which represents the leaf area per unit horizontal area of the canopy above the height z. Note that $L_{AI}(0) = L_{AI}$.

In most crop and grass canopies leaves are the most active and dominant elements of interaction with the atmosphere, and the fractional area represented by plant stems and branches can be neglected. Exceptions are certain forest canopies in which woody elements may not be ignored. Particularly for a deciduous forest in late fall and winter, the woody-element silhouette area index (W_{AI}), which can be defined in a manner similar to L_{AI}, is an important architectural characteristic. The sum of the two indices is called the plant area index

$$P_{AI} = L_{AI} + W_{AI} \tag{15.10}$$

Both the leaf area density and the leaf area index are found to vary over a wide range for the various crops and forests. For a particular crop, they also depend on the density of plants and their stage of growth. For illustration purposes, Figures 15.1 and 15.2 show their observed distributions in a deciduous forest canopy in summer months. Note that for this particular canopy, $L_{AI} \cong 4.9$, $W_{AI} \cong 0.6$, and $P_{AI} \cong 5.5$. Observations of the same parameters for other forest and crop canopies are reviewed by Monteith (1975, 1976).

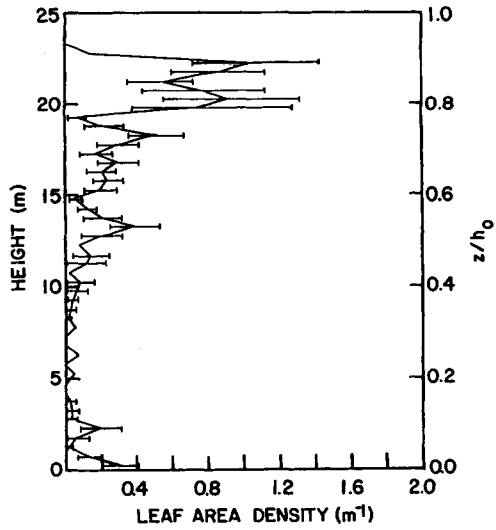

Figure 15.1 Vertical distribution of mean leaf area density in a deciduous forest in eastern Tennessee. [After Hutchinson *et al.* (1986).]

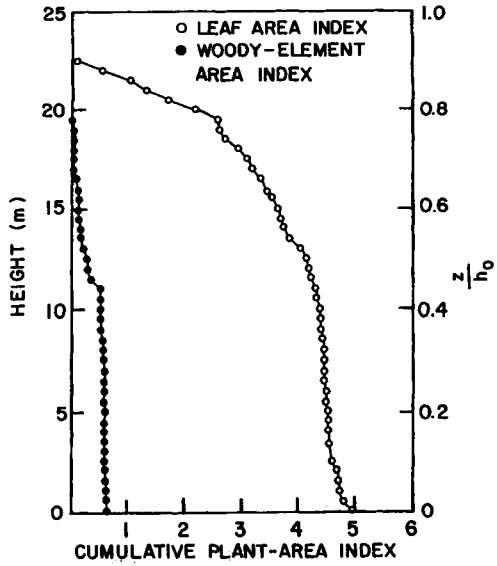

Figure 15.2 Vertical distribution of local cumulative leaf area index and woody element area index in a deciduous forest in eastern Tennessee. [After Hutchinson *et al.* (1986).]

The orientation of leaves is characterized by the mean leaf inclination angle from the horizontal. One can also measure the cumulative frequency distribution of the inclination angle. The foliage of many plant stands are more or less uniformly oriented, but some may display a narrow range of inclination angles around the horizontal, vertical, or somewhere in between (these are called panophile, erectophile and plagiophile canopies). A useful inclination index of the foliage is defined by Ross (1975). This index also depends on plant species and has a height and seasonal dependency.

15.2.2 Penetration of shortwave radiation

For a given incident solar radiation at the top of the canopy, the radiation regime in a plant canopy is determined by the canopy architecture, as well as by radiative properties of the various canopy elements and the ground surface. At any particular level in the canopy, the incoming solar radiation (both direct and diffuse) may vary considerably in the horizontal due to the presence of sunflecks and shadow areas with transitional areas, called penumbra, in between. Therefore, appropriate spatial averaging is necessary when we represent the radiative flux density as a function of height alone.

The transmission of incoming shortwave radiation into a plant canopy shows an approximately exponential decay with depth of penetration (more appropriately, the depth-dependent leaf area index), following the Beer–Bouguer law

$$R_{S\downarrow}(z) = R_{S\downarrow}(h_0)\exp[-\alpha L_{AI}(z)] \tag{15.11}$$

in which α is an extinction coefficient. The same law, perhaps with a slightly different value of extinction coefficient, applies to the net shortwave radiation. A comparison of observed profiles of incoming and net shortwave radiations in a grass canopy with Equation (15.11) is shown in Figure 15.3. The diurnal variation of the extinction coefficient for the same canopy is shown in Figure 15.4. Radiation measurements in forest canopies also show the approximate validity of Equation (15.11), with P_{AI} replacing L_{AI}.

Foliage in a canopy not only attenuates the radiative flux density but it also changes its spectral composition. Leaves absorb visible (PAR) radiation more strongly than they absorb the near infrared radiation (NIR). This selective absorption reduces the photosynthetic value of the solar radiation as it penetrates through greater depths in the canopy. The spectral composition of total radiation also differs in sunflecks and shaded areas; in sunflecks the spectrum is similar to that of the incident total radiation, while in shaded areas the NIR dominates.

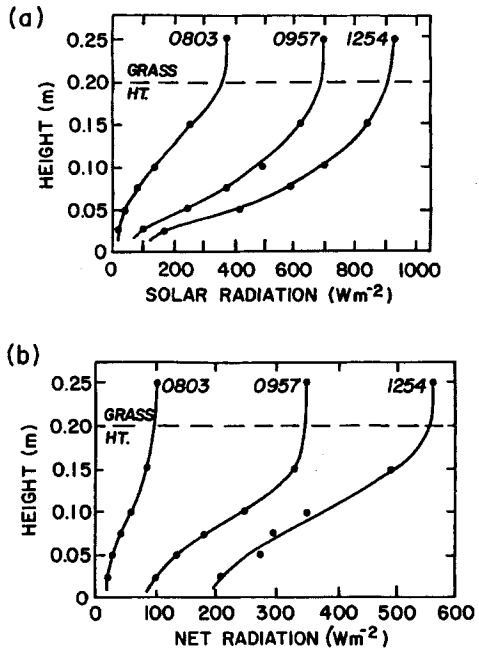

Figure 15.3 Observed profiles of (a) incoming solar radiation (R_S) and (b) net all-wave radiation (R_N) in a 0.2 m stand of native grass at Matador, Saskatchewan, on a clear summer day. [From Oke (1987); after Ripley and Redmann (1976).]

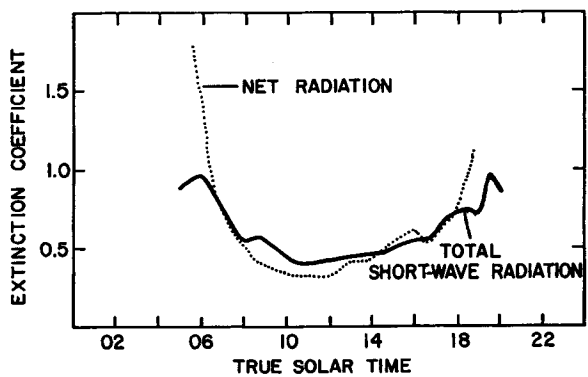

Figure 15.4 Diurnal variations of incoming solar and net radiation extinction coefficients for the native grass at Matador, Saskatchewan. [After Ripley and Redmann (1976).]

The shortwave reflectivity or albedo of a plant canopy depends on the average albedo of individual leaves, the canopy architecture (in particular, the canopy height, the leaf area index, and the leaf inclination index), and the solar altitude angle. The latter two factors determine the amount of penetration, radiation trapping, and mutual shading within the canopy. The longer the path of attenuation, the greater the amount of radiation to be trapped and the less to be reflected. Consequently, the albedo of most plant canopies is a decreasing function of both the canopy height and the solar altitude (Oke, 1987, Chapter 4).

15.2.3 Longwave radiation

The total or net longwave radiation (R_L) at any height within a plant canopy has four components: (1) the longwave radiation from the atmosphere which has penetrated through the upper layer of the canopy without interception; (2) the longwave radiation from the upper leaves and other canopy elements; (3) the radiation from lower canopy elements; and (4) the part of outgoing longwave radiation from the ground surface which is not intercepted by lower canopy elements. The net longwave radiation at the top of a plant canopy is almost always a loss, as with most other surfaces. However, the net loss usually diminishes toward the ground due to the reduction in the sky view factor (SVF), as the cold sky radiative sink is increasingly being replaced by relatively warmer vegetation surfaces. Consequently, in the lower part of a tall and dense canopy the role of sky becomes insignificant and R_L depends largely on the ground-surface temperature, the vertical distribution of mean foliage temperature, and ground and leaf surface emissivities. If the foliage temperature distribution is nearly uniform, which may be the usual case, R_L is also approximately constant, independent of height. The variation of R_L in the upper parts of the canopy is much more complicated (Ross, 1975).

15.3 Wind Distribution in Plant Canopies

Wind profiles above plant canopies ($z \geq 1.5h_0$) have been observed to follow the log law or the modified log law, depending on the atmospheric stability. Just above and within the canopy, however, the observed profiles deviate systematically (toward higher wind speeds) from the theoretical (modified log law) profile. The actual flow around roughness elements being three-dimensional, we can think of some generalized vertical profiles of wind and momentum flux only in a spatially averaged sense. With mechanical mixing processes dominating within the canopy, the stability effects can safely be ignored. If the large-scale

pressure gradients can also be ignored, as is commonly done in the above-canopy surface layer, the equations of motion degenerate to the usual condition that the divergence of the total vertical momentum flux must be zero. The main difference between the flow inside the canopy and that above it is that considerable momentum is absorbed over the depth of the canopy in the form of drag due to the various canopy elements.

An appropriate equation for horizontally averaged wind flow within a canopy is (Plate, 1971; Businger, 1975)

$$\partial \overline{uw}/\partial z = -(1/\rho)(\partial P/\partial x) - \tfrac{1}{2} C_d A U^2 \tag{15.12}$$

where C_d is the average drag coefficient of the plant elements and A is the effective aerodynamic surface area of the vegetation per unit volume. Both C_d and A are likely to be complicated functions of height and the canopy structure. When the pressure term is negligible, e.g., in the upper part of the canopy, Equation (15.12) reduces to

$$\partial \overline{uw}/\partial z = -\tfrac{1}{2} C_d A U^2 \tag{15.13}$$

Practical models of wind flow in canopy are based on the solution to Equation (15.13) with appropriate assumptions for C_d, A, and the relation between shear stress and mean velocity gradient (e.g., an eddy viscosity or a mixing-length hypothesis). Using the simplest assumption that C_d is independent of height and the mixing-length relation [Equation (9.21)] is valid with a constant l_m, the solution to Equation (15.13) is an exponential wind profile (Inoue, 1963)

$$U(z)/U(h_0) = \exp[-n(1 - z/h_0)] \tag{15.14}$$

where $U(h_0)$ is the wind speed at the top of the canopy and $n \equiv (C_d A/4l_m^2)^{1/3} h_0$.

An exponential profile similar to Equation (15.14) can also be derived from an eddy viscosity relation for momentum flux with an exponential variation of K_m which is consistent with a constant l_m (Thom, 1975). If, on the contrary, K_m is assumed constant, the resulting canopy wind profile is of the form

$$U(z)/U(h_0) = [1 + m(1 - z/h)]^{-2} \tag{15.15}$$

where m is a numerical coefficient characterizing the plant canopy. The actual difference in the profile shapes given by Equations (15.14) and (15.15) is small for the appropriate choice of profile parameters n and m (compare the two, for example, for $n = m = 3$), despite the strong contrast in the associated K_m profiles. This seems to indicate that the predicted canopy wind profile is not very sensitive to the assumed K_m or l_m distribution within reasonable limits.

The simplifications and assumptions used in the derivation of the exponential profile [Equation (15.14)] are such that one may wonder if it could represent the observed wind profiles in plant canopies. Surprisingly, however, a number of observed profiles do agree with Equation (15.14), especially in the upper half of canopies. This is partially because the parameter n is only weakly dependent on C_d and A. Figure 15.5 shows a comparison of some observed profiles in wheat and corn canopies with the exponential profile Equation (15.14). The data suggest that a unique (similarity) profile shape may exist for each canopy type. Cionco (1972) has summarized the best estimated empirical values of n for various canopies; they usually lie between 2 and 4. This simple theoretical or semiempirical model may represent only a part of the canopy wind profile. The model can be refined further by considering variations with height of C_d, A, and l_m (Cionco, 1965).

In a tall and well-developed canopy such as a mature forest, most of the momentum is absorbed in the upper part of the canopy where leaves are concentrated. Farther down, as the leaf area density decreases to zero, the pressure gradient term in Equation (15.12) is likely to become more significant and perhaps dominate over the flux-divergence term. Consequently, wind speed may increase with decreasing height above the ground, until surface friction reverses this trend close to the ground level. This suggests that a low-level wind maximum (jet) may appear in the lower part of certain forest canopies. This is indeed confirmed by many observations, a sample of which is shown in Figure 15.6. Note that a variety of wind profile shapes are found in forest canopies.

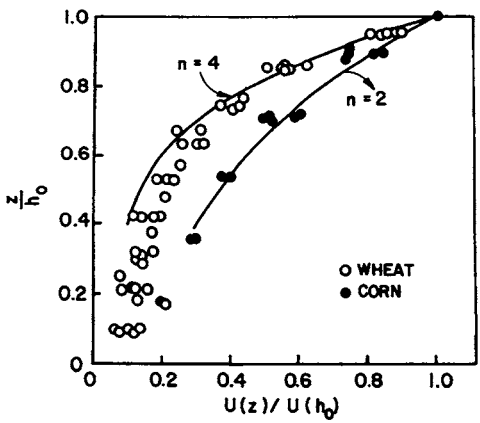

Figure 15.5 Comparison of observed mean velocity profiles in wheat and corn canopies with the exponential profile Equation (15.14) with $n = 4$ and 2, respectively. [After Plate (1971) and Businger (1975).]

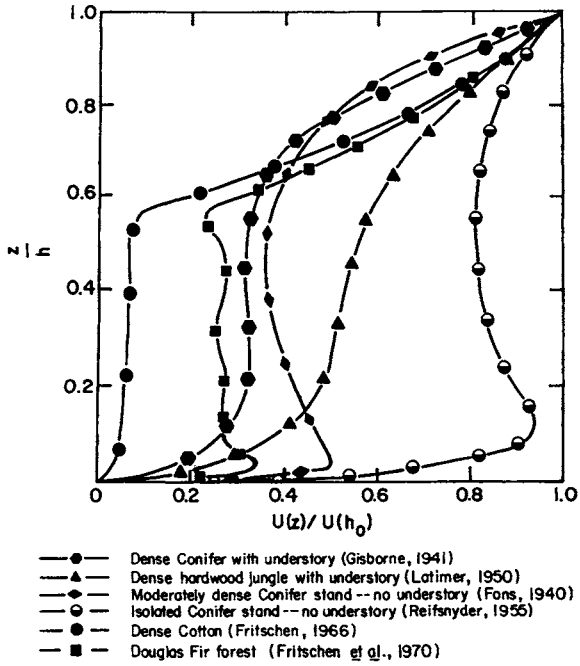

Figure 15.6 Observed mean wind profiles in different forest canopies. [From Businger (1975); after Fritschen *et al.* (1970).]

15.4 Temperature and Moisture Fields

Temperature profiles have been measured in various crop and forest canopies; these are quite different from those above the canopies. There are differences in canopy temperature profiles due to different canopy architectures. There are also significant diurnal variations in these due to variations of dominant energy fluxes. Here, we shall discuss only some typical observations and point out some of the common features of canopy temperature and humidity profiles. For a more comprehensive review of the literature the reader should refer to Monteith (1975, 1976).

Figure 15.7 shows the observed hourly averaged air temperature profiles within and above an irrigated soybean crop over the course of a day. Often, during daytime, there is a temperature maximum near middle to upper levels of the canopy. Since the sensible heat exchange in the canopy is expected to be down the temperature gradient, the heat flux is downward (negative) below the level of temperature maximum and upward (positive) above it. Thus, the sensible heat diverges away from the source region which coincides with the

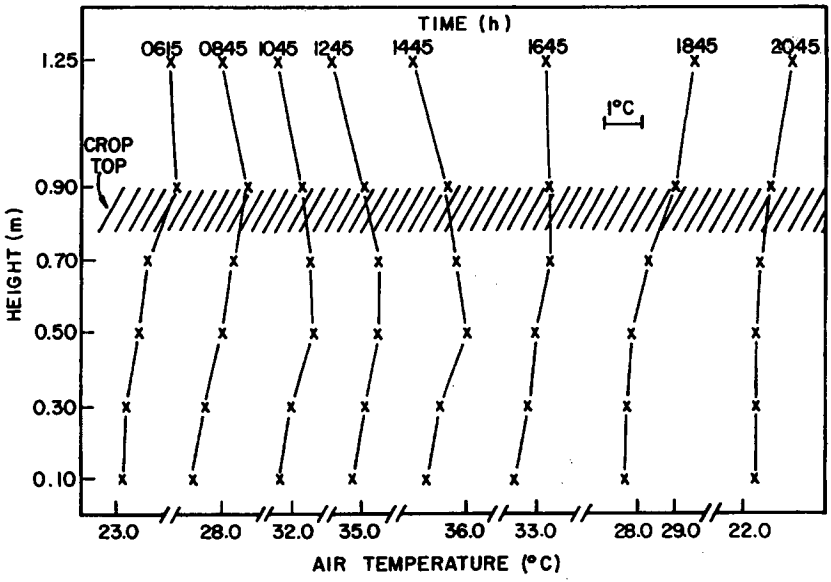

Figure 15.7 Mean air temperature profiles within and above an irrigated soybean crop on a summer day at Mead, Nebraska. [After Rosenberg *et al.* (1983).]

level of maximum leaf area density where most of the solar radiation is absorbed. The temperature inversion in the lower part of the canopy is a typical feature of daytime temperature profiles in tall crop and forest canopies. At night, temperature profiles in lower parts of canopies are close to isothermal, because canopies trap most of the outgoing longwave radiation. Often, the minimum temperature occurs not at the ground level but just below the crown. The nocturnal temperature inversion extends from above this level. The temperature gradient or inversion strength above a canopy is usually much smaller than that over a bare ground surface.

Figure 15.8 gives the hourly mean profiles of wind speed, temperature, water vapor pressure, and carbon dioxide inside and above a barley canopy on a summer day, for which the observed canopy energy budget is given in Figure 2.4. The observed wind and temperature profiles display the same features as discussed above. The daytime profiles of water vapor pressure show the expected decrease with height through much of the canopy and the surface layer above; a slight increase (inversion) in the upper part of the canopy is probably due to increased transpiration from the leaves in that region. Note that both the soil surface and foliage are moisture sources. The nocturnal vapor pressure profiles are more complicated by the processes of dewfall and guttation on leaves, while weak evaporation may continue from the soil surface.

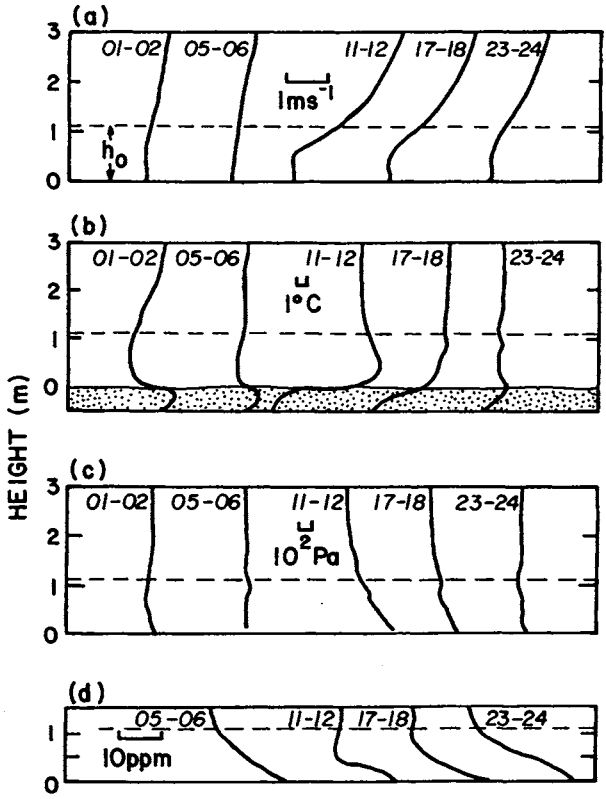

Figure 15.8 Observed profiles of (a) wind speed, (b) temperature, (c) water vapor pressure, and (d) carbon dioxide concentration in and above a barley crop on a summer day at Rothamsted, England. [From Oke (1987) after Long *et al.* (1964).]

Temperature and water vapor pressure profiles in forest canopies are similar to those within tall crops. The main difference is that the gradients are much weaker and diurnal variations are smaller in forest canopies. Even on warm, sunny days, air is cooler and more humid inside forests. Figure 15.9 presents the typical daytime profiles of meteorological variables and foliage area density. Both the temperature and the water vapor pressure profiles show maximum values at the level of maximum foliage density where the sources of heat (radiative absorption) and water vapor (transpiration) are most concentrated. Beneath this there is a temperature inversion, but nearly uniform vapor pressure profile; an inversion in the latter would be expected if the forest floor were dry. At night the temperature profile (not shown) is reversed, with a minimum occurring near the level of maximum foliage density. Due to reduced sky view

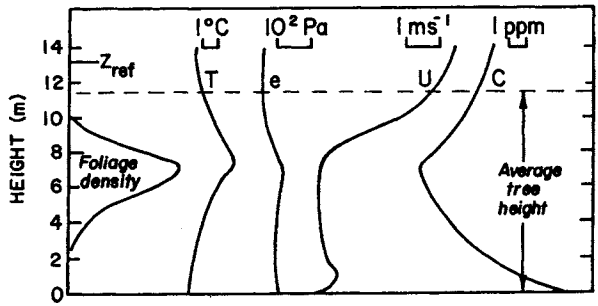

Figure 15.9 Observed mean profiles of foliage density and meteorological variables in a Sitka spruce forest on a sunny summer day near Aberdeen, Scotland. [After Jarvis *et al.* (1976).]

factor and trapping of longwave radiation in the lower part of the canopy, temperatures remain mild there, compared to those in open areas. Dewfall, if any, is largely confined to the upper part of the canopy, just below the crown. In the absence of dewfall, specific humidity or water vapor pressure is a decreasing function of height with weak evaporation from the soil surface as the only source of water vapor in the canopy.

15.5 Turbulence in and above Plant Canopies

The generation of turbulence in a plant canopy is a much more complex process than that over a flat bare surface or in a homogeneous boundary layer above a plant canopy. In addition to the usual sources of turbulence, such as mean wind shear and buoyancy, each canopy element is a source of turbulence due to its interaction with the flow and generation of separated shear layer and wake. The wake-generated turbulence in the canopy has characteristic large-eddy scales comparable to the characteristic sizes of the various canopy elements (e.g., leaves, branches and trunk). These scales are usually much smaller than the large-eddy scales of turbulence ($z - d_0$ and $h - d_0$) above the canopy. However, large-scale turbulence also finds its way through the canopy intermittently during short periods of downsweeps bringing in higher momentum fluid from the overlying boundary layer. It has been observed that the bulk of turbulent exchange between the atmosphere and a canopy may be occurring during these large-scale downsweeps and compensating low-momentum ejections or bursts of high turbulence. Thus, canopy turbulence is distinguished by a multiplicity of scales and generating mechanisms. It is also characterized by high-turbulence intensities, with turbulent velocity fluctuations of the same order or even larger than the mean velocity. These characteristics make canopy

turbulence not only extremely difficult to measure, but also preclude a simple representation of it in a similarity form. Still, for convenience, the height above the surface is usually normalized by the canopy height and σ_u, σ_v, σ_w are normalized by the mean wind speed at the measurement height or by the friction velocity u_* based on the momentum flux in the constant flux layer above the canopy.

15.5.1 Turbulence intensities and variances

Limited observations of longitudinal turbulence intensity $i_u = \sigma_u/U$ suggest that, typically, $i_u \cong 0.4$ in agronomic crops, 0.6 in temperate forests and between 0.7 and 1.2 in tropical forests (Raupach and Thom, 1981). In a gross sense, i_u increases with canopy density. The turbulence intensity profiles broadly follow the leaf or plant area density profiles, but are also influenced by mean wind speed and stability within the canopy. The lateral and vertical turbulence intensities (i_v and i_w) are generally proportional to but smaller than i_u. A comparison of turbulence intensity profiles within rice and corn canopies shows that the profile is nearly uniform in the former, with an approximately uniform leaf area density distribution, while the profile in the corn canopy has a maximum near the top of the canopy (Uchijima, 1976). More recent measurements of turbulence in a corn canopy also indicate increasing turbulence activity with height. For example, Figure 15.10 shows the profiles of normalized standard deviations of horizontal and vertical velocity components observed by Wilson *et al.* (1982).

Measurements of turbulence within and above forest canopies have been reported by Bergstrom and Hogstrom (1989) and Leclerc *et al.* (1990). The former study over a pine forest indicates that the turbulence kinetic energy (TKE) remains approximately constant within the height interval ($h_0 < z < 2.4h_0$, where $h_0 = 20$ m is the height of the trees at the location of the measurement tower) studied. The influence of atmospheric stability, as measured by h_0/L within a deciduous forest canopy and $(z - d_0)/L$ above the canopy, on the TKE budget is examined by Leclerc *et al.* (1990). They show that buoyancy effects (production or destruction of TKE) are largest in the upper third of the canopy where the foliage is densest and the radiation load highest. The magnitude of the buoyant production term increases almost linearly with increasing instability in the upper region of the canopy. The onset of stability exerts a strong influence on the shear production of the TKE. Both the shear and buoyancy terms become small in the lower half of the canopy; in strong stratification the former also becomes slightly negative. Within the canopy, turbulence is largely produced in the wakes of individual trees and branches.

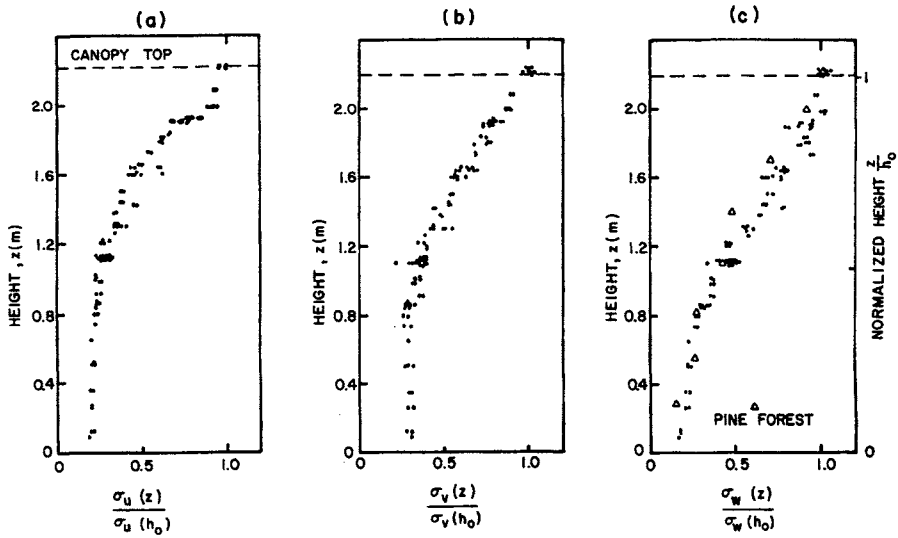

Figure 15.10 Observed profiles of the normalized standard deviations of (a) longitudinal, (b) lateral, and (c) vertical velocity fluctuations in a corn canopy. [After Wilson *et al.* (1982). Copyright © (1982) by D. Reidel Publishing Company. Reprinted by permission.]

15.5.2 Turbulent fluxes

Direct measurements of turbulent fluxes of momentum, heat, and water vapor are extremely difficult to make in plant canopies, and a few attempts have been made only recently. Figures 15.11 and 15.12 show some eddy correlation measurements of momentum and heat fluxes in a corn canopy. In general, fluxes increase with height and reach their maximum values somewhere near the top of the canopy. Their normalized profiles also show some day-to-day variations.

Only a few direct (eddy correlation) measurements of the turbulent fluxes of momentum, sensible heat, and water vapor above forest canopies have been reported in the literature (Verma *et al.*, 1986; Bergstrom and Hogstrom, 1989). Turbulent fluxes are found to remain practically constant (independent of height) in the height interval ($h_0 < z < 2.4h_0$) studied, which includes the roughness sublayer.

More often, turbulent fluxes are estimated from the observed mean profiles using gradient-transport hypotheses (e.g., eddy viscosity or mixing length). This approach suffers from many conceptual and practical limitations, however, and its validity has been seriously questioned by micrometeorologists in recent years (Raupach and Thom, 1981). It has been shown that vertical fluxes in plant

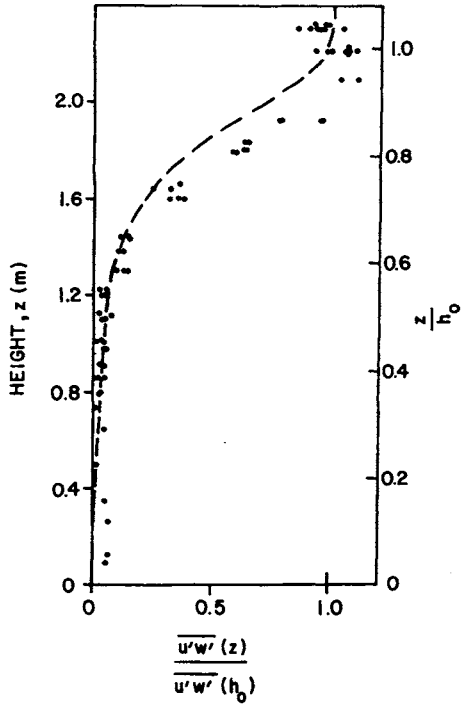

Figure 15.11 Measured and calculated profiles of normalized shear stress in a corn canopy. [After Wilson *et al.* (1982). Copyright © (1982) by D. Reidel Publishing Company. Reprinted by permission.]

canopies are not always down the mean vertical gradients, as implied in simpler gradient-transport hypotheses. For example, the vertical momentum flux $\overline{uw}$ may be driven by the horizontal gradient of mean vertical velocity ($\partial W/\partial x$) and/or by buoyancy, and need not be uniquely related to $\partial U/\partial z$. Even when it can be related to the latter through an eddy viscosity or a mixing-length relationship, the specification of K_m or l_m is not straightforward. A number of mutually contradictory K_m and l_m profiles have been proposed in the literature and there is much confusion regarding the shapes of flux profiles. There are very few direct observations of fluxes and gradients in canopy flows which support the gradient-transport (K) theories. On the contrary, observations show strong evidence for countergradient fluxes. Local-diffusion theories cannot cope with and predict such countergradient fluxes. The main reasons for their failure in canopy flow are three-dimensionality of the mean motion, nonlocal production of turbulence, and the multiplicity of the scales of turbulence.

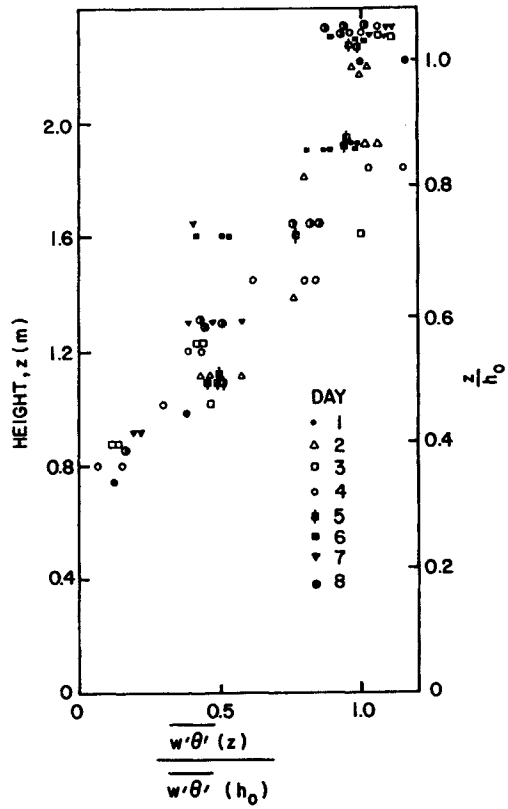

Figure 15.12 Daily normalized sensible heat flux profiles from eddy correlation measurements in a corn canopy. [After Wilson *et al.* (1982). Copyright © (1982) by D. Reidel Publishing Company. Reprinted by permission.]

A far better method of estimating turbulent transport or fluxes from measurements of mean wind, temperature, etc., inside canopies is based on the integration of mean momentum and other conservation equations with respect to height. For example, integration of Equation (15.13) yields

$$\frac{\overline{uw}(z) - \overline{uw}(0)}{\overline{uw}(h_0) - \overline{uw}(0)} = \frac{\int_0^z C_d A U^2 dz}{\int_0^{h_0} C_d A U^2 dz} \tag{15.16}$$

in which the integrals can be numerically evaluated for the given (measured) U profile, the leaf area density $A(z)$, and the average drag coefficient $C_d(z)$. The flux $\overline{uw}(0)$ at the canopy floor can usually be neglected. With this assumption, Equation (15.16) is compared with the observed profile in Figure 15.11. The

most uncertain parameter in this indirect estimation of momentum flux is the canopy drag coefficient C_d, which is known only for certain idealized plant shapes such as a circular cylinder.

Similar relationships can be derived for sensible heat and water vapor fluxes, using their appropriate conservation equations for the canopy layer. Figures 15.13 and 15.14 show the observed profiles of soil and air temperatures and water vapor pressure, together with the calculated profiles of sensible and latent heat fluxes in a grass canopy ($h_0 \cong 0.17$ m). Radiative fluxes within this canopy for the same day are given in Figure 15.3. Note that all the fluxes increase with height and attain their maximum values just above the canopy. During the late morning period the sensible heat flux is negative in the shallow surface inversion

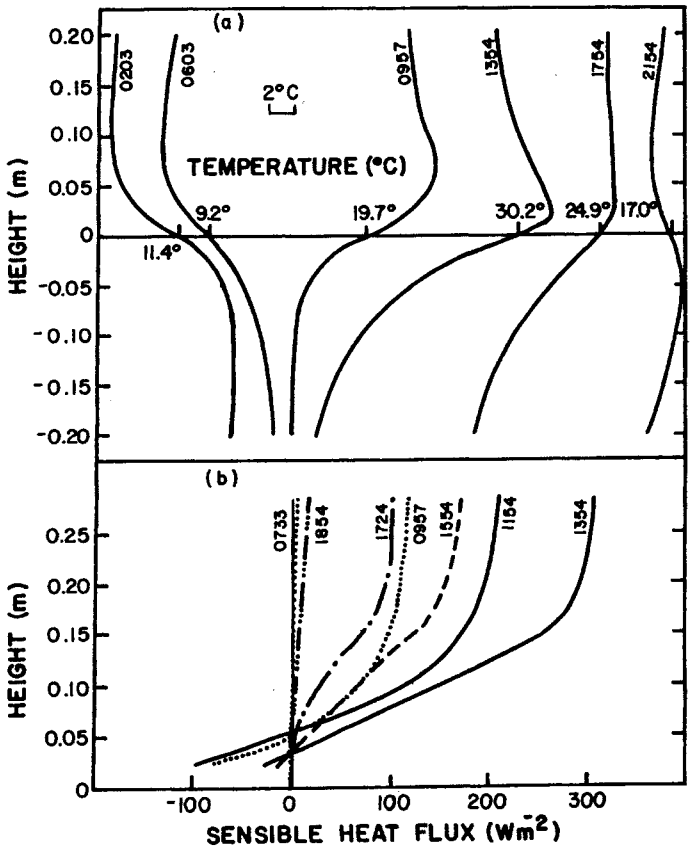

Figure 15.13 Observed profiles of (a) temperature in the canopy and upper layer of soil and (b) calculated profiles of sensible heat flux in a grass canopy at various times during a summer day. [After Ripley and Redmann (1976).]

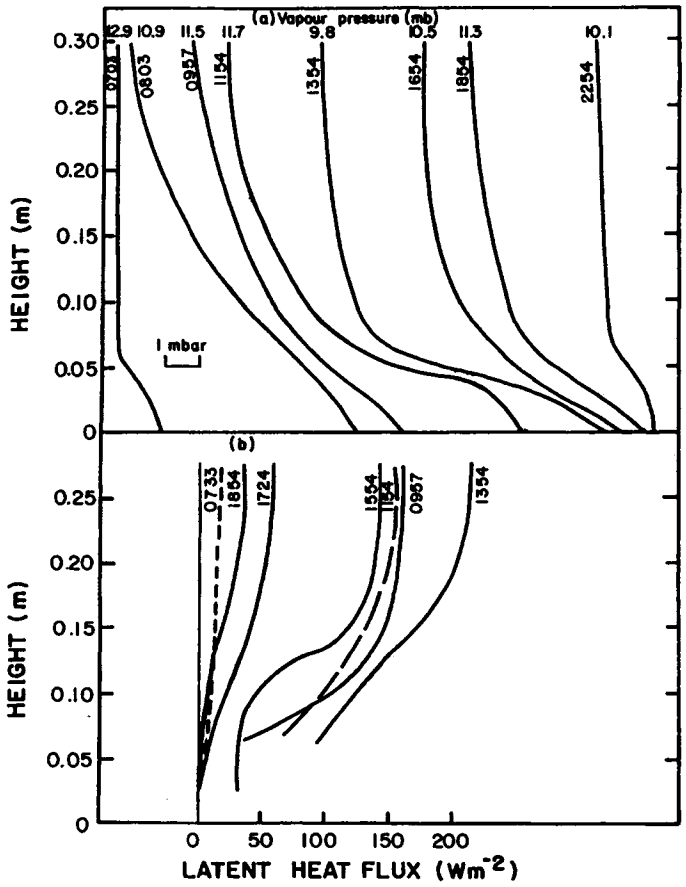

Figure 15.14 Observed profiles of (a) water vapor pressure (in millibars) and (b) calculated profiles of latent heat flux in a grass canopy at various times during a summer day. [After Ripley and Redmann (1976).]

layer that is destroyed later in the afternoon. This inversion in the lower part of the canopy probably produces a build-up of water vapor in this region during the morning period (see Figure 15.14a). The decrease in vapor pressure in early afternoon is a result of more vigorous turbulent mixing, bringing in drier air from higher levels. The highest vapor pressure occurs at the moist ground surface. The computed latent heat flux profiles in Figure 15.14b indicate that the major source region is around $z = d_0 \cong 0.10$ m in the morning and somewhat higher during the afternoon (Ripley and Redman, 1976).

The calculated profiles of eddy diffusivities of heat and momentum based on the above observations in a grass canopy during the morning period are shown

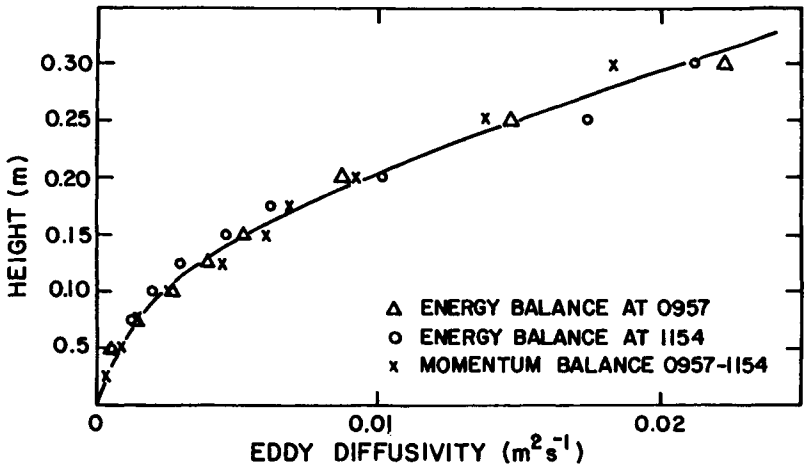

Figure 15.15 Vertical profiles of eddy diffusivity in a grass canopy calculated by the energy-balance and momentum-balance methods. [After Ripley and Redmann (1976).]

in Figure 15.15. Within the canopy the estimated values of K_h and K_m are in close agreement, indicating the dominance of mechanically generated turbulence in the canopy layer. Above the canopy ($z > h_0 \cong 0.17$ m), however, K_h values increase more rapidly with height than K_m values, which might be expected from increasing buoyancy effects on turbulence. These are probably the most consistent estimates of eddy diffusivities in a canopy flow, suggesting the usefulness and validity of gradient-transport relations, at least in a thin grasslike canopy. The observation that other periods of the day did not show such a good agreement cautions against any broad generalization of such results.

15.6 Applications

A primary objective of the various micrometeorological studies involving plant canopies has been to better understand the processes of momentum, heat, and mass exchanges between the atmosphere and the biologically active canopy. These exchanges influence the local weather as well as the microclimate in which plants grow. A basic understanding of exchange mechanisms and subsequent development of practical methods of parameterizing them in terms of more easily and routinely measured parameters is essential for many applications in meteorology, agriculture, forestry, and hydrology. More specific applications of agricultural and forest micrometeorology are as follows:

- Determining the mean wind, temperature, humidity, and carbon dioxide profiles in and above a plant cover.
- Determining the radiative and other energy fluxes in a plant cover.
- Predicting the ground surface and soil temperatures and moisture content.
- Estimating evaporation and transpiration losses in plant canopies.
- Determining photosynthetic activity and carbon dioxide exchange between plants and the atmosphere.
- Protection of vegetation from strong winds and extreme temperature.

Problems and Exercises

1. Explain the concept and physical significance of the zero-plane displacement. How is it related to the height and structure of a plant canopy?

2.

(a) Show that the aerodynamic resistance of a plant canopy in a stably stratified surface layer is given by

$$r_M = r_H = \frac{1}{ku_*}\left[\ln\left(\frac{z-d_0}{z_0}\right) + \beta\left(\frac{z-d_0}{L}\right)\right]$$

(b) Plot r_M as a function of the normalized height for the values of $u_* = 0.25$, 0.50, 0.75, and 1.0 m s^{-1} in neutral conditions.

(c) How does atmospheric stability affect the aerodynamic resistance?

3.

(a) Using the Bear–Bouguer law express the net all-wave radiation (R_N) as a function of height for a constant leaf area density canopy of height h_0.

(b) For the same canopy, plot $R_N(z)/R_N(h_0)$ as a function of z/h_0 for different values of the extinction coefficient $\alpha = 0.5$, 0.75, and 1.0.

(c) How is the net longwave radiation expected to vary with height in such a canopy?

4.

(a) Using Equation (15.13) and the mixing-length relation for $\overline{uw}$ with a constant mixing length l_m, derive the exponential wind profile [Equation (15.14)] for the canopy flow.

(b) Derive an expression for eddy viscosity K_m for the same flow.

(c) Plot $U(z)/U(h_0)$ as a function of z/h_0 for different values of the parameter $n = 1$, 2, 3, and 4.

5.

(a) Using the eddy viscosity relation for $\overline{uw}$ with a constant K_m, derive the canopy wind profile Equation (15.15).

(b) Compare the wind profiles given by Equations (15.14) and (15.15) for $n = m = 3$.

6.

(a) Why do the fluxes of momentum, heat, and water vapor generally increase with height in a plant canopy?

(b) Derive an expression for the momentum flux profile in a uniform plant area density canopy for the given exponential wind profile, Equation (15.14).